

A Passively Growing Sheath for Reducing Friction of Linearly Moving Structures

Hanbeom Seo, Dongki Kim, Gwang-Pil Jung*

Mechanical and Automotive Engineering, Seoul National University of Science and Technology, Seoul, Republic of Korea

*Corresponding author: Gwang-Pil Jung, gpjung@seoultech.ac.kr

Copyright: © 2023 Author(s). This is an open-access article distributed under the terms of the Creative Commons Attribution License (CC BY 4.0), permitting distribution and reproduction in any medium, provided the original work is cited.

Abstract

A linearly moving structure in the area where the friction force is dominant, such as ducts filled with grease in the nuclear power plant, experiences an increase in friction since the contact surface gets larger as the structure proceeds. To solve this problem is critical for the pipe inspection robot to investigate further areas and this makes the system more energy-efficient. In this paper, we propose a passively growing sheath that can be added to linearly moving structures using a zipper mechanism. The mechanism enables the linearly moving structures to maintain rolling contact conditions against the external environment, which provides a substantial reduction in kinetic friction. To analyze the effect of the mechanism's head shape, a physical model was established and compared to the experimental results in this study. Finally, the passively growing sheath was shown to be successfully applied to the pipe inspection robot for the nuclear power plant.

Keywords

Growing robot
Reducing friction
Zipper mechanism
Pipe inspection

1. Introduction

This study describes the friction reduction structure of a robot for determining the corrosion of steel inside ducts filled with grease to protect steel structures in nuclear power plants [Figure 1(a)]. Currently, the process of determining the corrosion of steel involves removing all the grease, removing the steel, and performing a visual inspection after relieving the stress in the steel. This process consumes a lot of time and resources. Therefore, a robot capable of effectively moving in

a viscous environment can replace this inefficient inspection method and also create various applications such as maintenance and reinforcement.

In this research group, a linear actuator-type inspection robot is used to move inside the duct [Figure 1(b)]. Such linear robots experience viscous friction due to the relative motion between the actuator unit and the grease during movement inside the grease, and the magnitude of this friction increases continuously with the robot's movement distance and speed. For example,

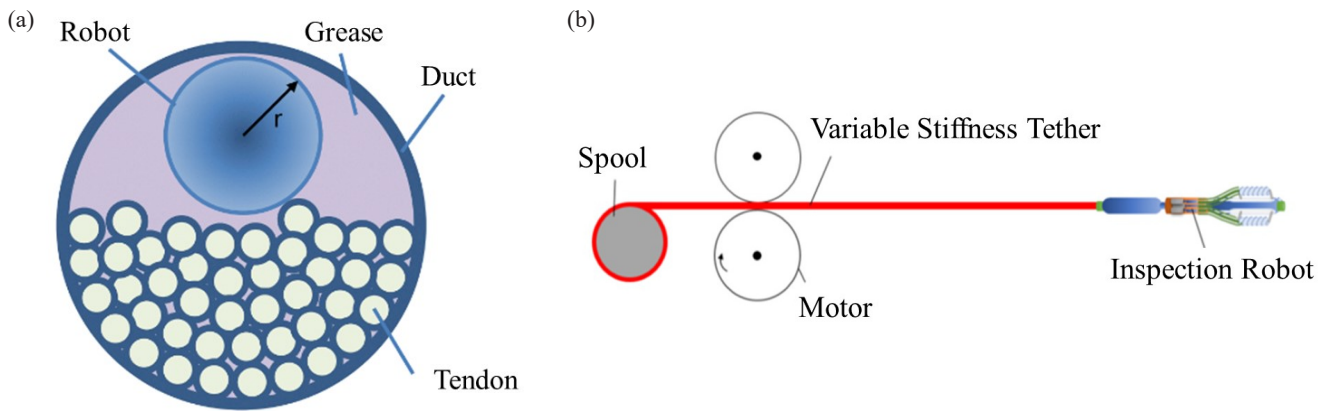


Figure 1. (a) Diagram of the nuclear power plant duct, (b) a linear inspection system.

assuming that the linear actuator used in this paper moves at 0.01 m/s when the duct is moved 100 m, the viscous friction reaches 180 kg, requiring a high-power actuator motor and transmission. Therefore, solving the increasing viscous friction problem is essential to lighten the system and increase the actuator efficiency.

The tip elongation characteristic of plant roots minimizes relative movement and interaction with the external environment through end growth without overall structure movement ^[1], hence applying this to linear actuators can solve the aforementioned problem. The recently popular Soft Vine Robot effectively mimics this characteristic through pneumatic means, moving effectively in constrained environments and presenting various possibilities ^[2-5]. However, the enclosed pneumatic system presents difficulties in directly applying the Vine Robot to the aforementioned inspection robot.

Thus, if the tip growth characteristics can be modularized and added to the existing system, the friction reduction characteristic can be flexibly applied as needed, and the existing robot can be used more flexibly. Hence, this paper proposes a modular friction reduction passive growth sheath design through a zipper mechanism and conducts a comparative analysis through simple modeling and design parameter experiments. This paper is organized as follows: Section 2 introduces the system design and operation

method, Section 3 presents the modeling, Section 4 presents the experiments and results, and finally, Section 5 describes the conclusion and future plans.

2. Design

2.1. Conceptual design

The schematic configuration of this system is shown in **Figure 2(a)**. One end of the nylon membrane is anchored and stored on a spool. When the linear actuator moves forward, the head attached to the actuator unit moves along with it and pulls the membrane stored on the spool. The pulled membrane (tail) passes through the head, forming a new outer wall that encompasses the entire system, causing the tip to grow. Therefore, the new membrane unfolds through rolling conditions at the end of the linear actuator with minimal friction, allowing movement without relative displacement of the entire system.

The main mechanism of this paper is the covering transition from an open state to a closed state that completely encloses the linear actuator through the head, allowing the membrane to be added to the linear actuator system as a separate system. This was implemented using a zipper mechanism [**Figure 2(b)**].

In the duct environment assumed in this study, the approximate diameter through which the robot can pass on the steel wire is 0.1 m, and to minimize resistance when moving inside the grease, it was manufactured

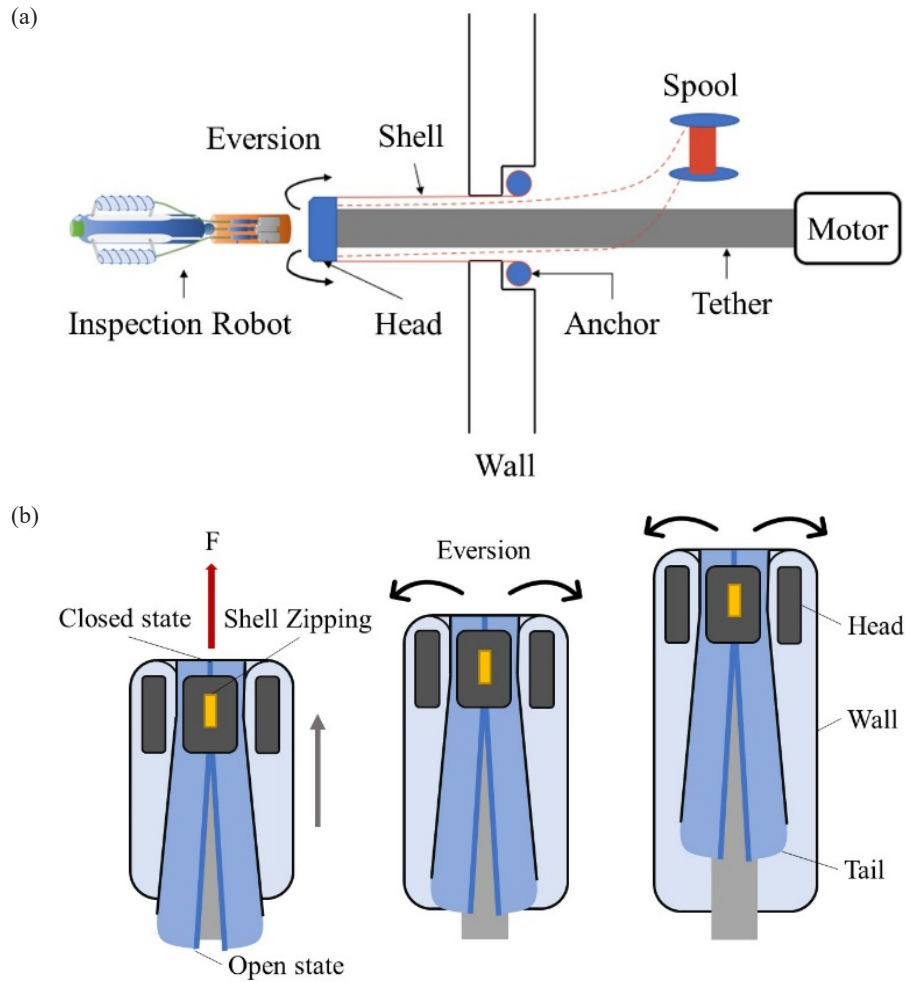


Figure 2. (a) Integrated system diagram, (b) eversion process using zipper mechanism

with a diameter similar to that of the inspection robot to be attached to the front, which is 0.05 m.

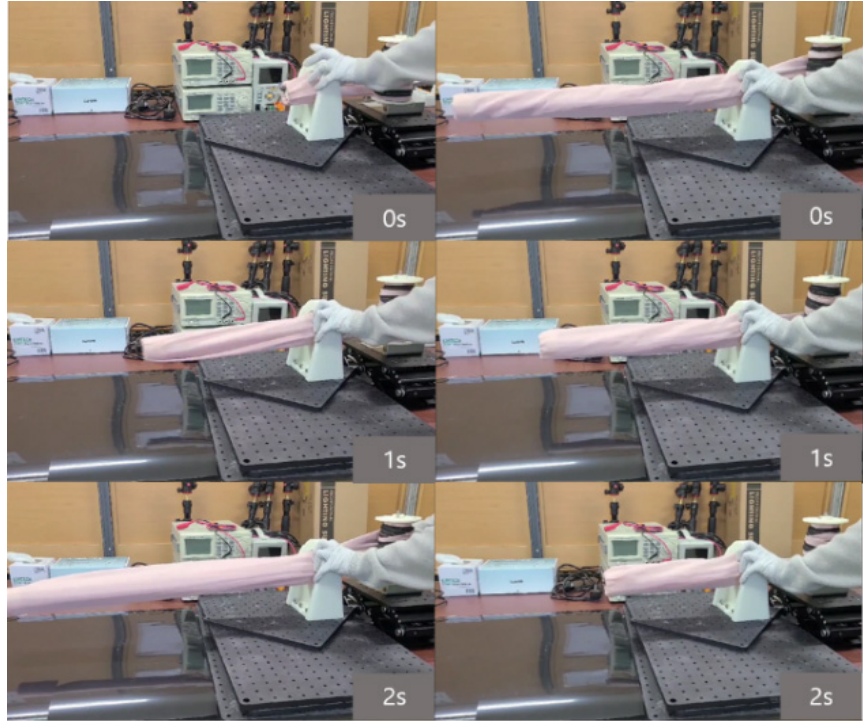
2.2. Operating method

This system grows using the propulsion of the linear actuator during growth and is retracted using the restoring force of the constant-load spring attached to the spool (**Figure 3**). The constant-load spring exhibits a consistent torque output after an initial displacement, providing significant advantages over conventional springs in a system designed for substantial length movement.

The region where the tip grows and zipping occurs is divided into the coupling structure that attaches to the actuator and the portion where the covering

transitions from tail to wall. The design of the coupling structure is variable depending on the form of the linear actuator, and in this paper, a friction-enhancing polymer was attached between the actuator and the head, then secured with screws to integrate it into the existing actuator system. The covering moves along a ring-shaped structure surrounding the support structure and transitions from tail to wall. During the unfolding of the covering, if there is too much slack in the covering, the covering may get stuck in the zipper or wrinkle, causing interference with the attachment. This is minimized by positioning the zipper on the outer surface of the head, where there is relatively less slack in the covering.

Figure 3. Growing process (left), and retracting process (right)



3. Modeling

The existing Soft Vine Robot experiences force losses during the membrane transfer process from the spool and the eversion process of the covering, which can be formulated as follows ^[6]:

$$PA = [Path\ Independent] + [Path\ Dependent] \quad (1)$$

$$PA = \left[YA + \left(\frac{1}{\varphi} v \right)^{\frac{1}{n}} A \right] + \left[\mu_s wL + \sum_i C e^{\frac{\mu_c L_i}{R_i}} \right] \quad (2)$$

The mechanism in this paper unfolds through linear drive forces, similar to the Soft Vine Robot mentioned above. Therefore, assuming linearity in the relationship between forces, equation (2) can be transformed and applied as follows:

$$F = [F_{anchor} + F_{zip} + F_{spring}] + \left[\mu_s wL + \sum_i C e^{\frac{\mu_c L_i}{R_i}} \right] \quad (3)$$

Here, F_{anchor} represents the force exerted on the covering from the anchor, F_{zip} is the force for zipper attachment, and F_{spring} is the restoring force of the spool. Assuming very low friction between the coverings, the relatively small $[Path\ Dependent]$ term

can be eliminated during linear drive motion ^[7], which is simplified as follows:

$$F = [F_{anchor} + F_{zip} + F_{spring}] \quad (4)$$

The friction behavior between the head and the covering during the eversion process can be described as a kind of motion between a capstan and a rope (**Figure 4**), and similar to the capstan equation (5), the relationship between F_{anchor} and F_{spring} can be expressed as a coefficient of $k(\mu_s, \theta)$ (6).

$$T_{Load} = T_{Hold} \times e^{\mu_s \theta} \quad (5)$$

$$F_{anchor} = F_{spring} \times k(\mu_s, \theta) \quad (6)$$

Here, θ is the contact angle between the head and the covering, and μ_s is the friction coefficient between the head and the covering. Therefore, the force required for the system to grow can be expressed as follows:

$$F = F_{zip} + (1 + k) \times F_{spring} \quad (7)$$

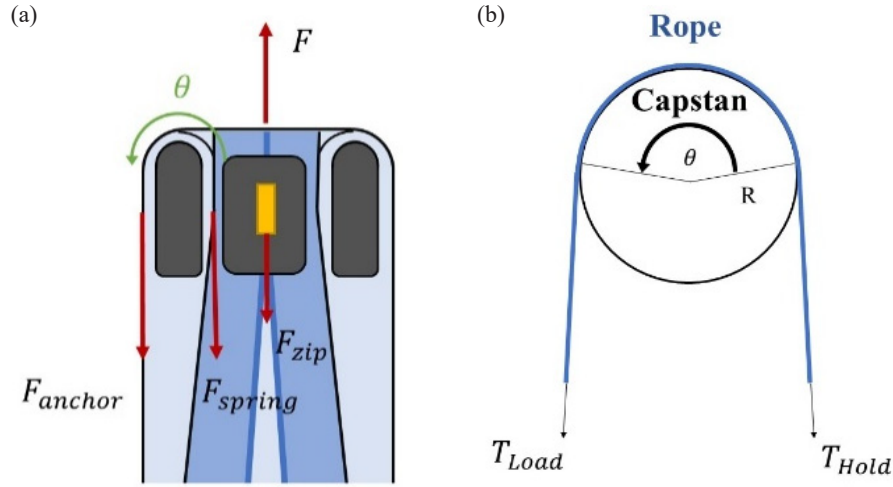


Figure 4. (a) System modeling, (b) capstan equation diagram

4. Experiments and results

4.1. Comparison of modeling and experimental values

In this paper, the values of F_{model} obtained by substituting the experimentally determined values of F_{zip} and $k(\mu_s, \theta)$ into equation (7) were compared with F_{exp} obtained through integrated experiments. The modeling results were tested for three different contact angles: $\theta=150^\circ$, $\theta=180^\circ$, and $\theta=230^\circ$. The values of each term obtained through experiments are shown in **Table 1**.

F_{zip} was measured as the force required for zipper attachment after securing the covering, and F_{spring} was measured as the force required to unroll the covering from a spool with 6 m of covering stored. k was measured by applying a load to one end while

fixing the other end, causing the head to experience friction with the covering and move at a constant speed, as shown in **Figure 5**. The value of k was determined through the process outlined in equations (8) to (11), and the average values were calculated for T_{load} at 10 N, 14 N, and 20 N, respectively. All of the above experiments were conducted with three replicates each, and the results are presented in **Table 2**.

$$T_{hold} = T_{load} \times k \quad (8)$$

$$F_{measure} = T_{load} + T_{hold} \quad (9)$$

$$F_{measure} = (1 + k) \times T_{load} \quad (10)$$

$$k = \frac{F_{measure}}{T_{load}} - 1 \quad (11)$$

Table 1. Experiment results0

	$\theta=150^\circ$	$\theta=180^\circ$	$\theta=230^\circ$
F_{zip}		1.5 N	
F_{spring}		6.5 N	
k	3.7	3.42	5.14
F_{model}	32.05 N	30.23 N	41.41 N
F_{exp}	39 N	34.3 N	51.6 N
ERROR	17.8%	11.9%	19.8%

Table 2. k data results

	10 N	14 N	20 N	Average
$k_{\theta=150^\circ}$	3.85	3.86	3.4	3.7
$k_{\theta=180^\circ}$	3.46	3.5	3.3	3.42
$k_{\theta=230^\circ}$	5.31	5.13	4.99	5.14

**Figure 6.** integration test with a linear actuator

The modeling values and experimental values showed errors of 17.8%, 11.9%, and 19.8% at $\theta=150^\circ$, $\theta=180^\circ$, and $\theta=230^\circ$, respectively. This discrepancy is due to the wrinkling of the covering and misalignment between the zipper and covering, as well as the *[Path Dependent]* term arising from actual covering behavior.

For $k(\mu_s, \theta)$, it was observed that k at $\theta=230^\circ$ is 50% larger than $k_{\theta=180^\circ}$, indicating a tendency for optimized k values depending on the contact angle. Unlike the conventional capstan equation, k is influenced by factors such as the wrinkling of the covering, the clearance between the covering and the head, in addition to the contact angle and friction coefficient. As a result, the actual motion of the covering involves three-dimensional surface friction, and the head is not entirely structurally similar to a capstan, leading to these variations.

4.2. System integration testing

Based on the results of this experiment, the system integration test was conducted with the $\theta=180^\circ$ design,

which requires the least force for system growth. It was confirmed that the covering successfully grew and retracted with the linear actuator, and the mechanism operated as intended (**Figure 6**).

5. Conclusion

In this paper, a mechanism was proposed for the efficient movement of structures that linearly move in spaces where viscous friction is significant. Additionally, a comparative analysis of the growth force was conducted based on the shape of the head through simple modeling and experiments. Through this, it is expected that in future research, the system can be improved with a more optimized head design and minimizing F_{spring} during growth. The actual integration experiment with the linear actuator confirmed the successful operation of this mechanism, and the modular design can potentially be used for various purposes in structures that move linearly, beyond the linear actuator used in this study.

Disclosure statement

The authors declare no conflict of interest.

Acknowledgment

This work was supported by the Korean Hydro & Nuclear Power Co., Ltd (KHNP).

References

- [1] Sadeghi A, Mondini A, Mazzolai B, 2017, Toward Self-Growing Soft Robots Inspired by Plant Roots and Based on Additive Manufacturing Technologies. *Soft Robotics*, 4(3): 211–223. <https://doi.org/10.1089/soro.2016.0080>
- [2] Hawkes EW, Blumenschein LH, Greer JD, et al., 2017, A Soft Robot that Navigates Its Environment Through Growth. *Science Robotics*, 2(8). <https://doi.org/10.1126/scirobotics.aan3028>
- [3] Jeong S-G, Coad MM, Blumenschein LH, et al. 2020 IEEE/RSJ International Conference on Intelligent Robots and Systems (IROS), October 25–29, 2020: A Tip Mount for Transporting Sensors and Tools using Soft Growing Robots. 2020, Las Vegas. <https://doi.org/10.1109/IROS45743.2020.9340950>
- [4] Stroppa F, Luo M, Yoshida K, et al. 2020 IEEE International Conference on Robotics and Automation (ICRA), May 31–August 31, 2020: Human Interface for Teleoperated Object Manipulation with a Soft Growing Robot. 2020, Paris. <https://doi.org/10.1109/ICRA40945.2020.9197094>
- [5] Kim J-H, Jang J, Lee S-M, et al., 2021, Origami-Inspired New Material Feeding Mechanism for Soft Growing Robots to Keep the Camera Stay at the Tip by Securing its Path. *IEEE Robotics and Automation Letters*, 6(3): 4592–4599. <https://doi.org/10.1109/LRA.2021.3068936>
- [6] Blumenschein LH, Okamura AM, Hawkes EW, 2017, Modeling of Bioinspired Apical Extension in a Soft Robot. *Conference on Biomimetic and Biohybrid Systems*, 2017: 522–531. https://doi.org/10.1007/978-3-319-63537-8_45
- [7] Haggerty DA, Naclerio ND, Hawkes EW, 2021, Hybrid Vine Robot with Internal Steering-Reeling Mechanism Enhances System-Level Capabilities. *IEEE Robotics and Automation Letters*, 6(3): 5437–5444. <https://doi.org/10.1109/LRA.2021.3072858>

Publisher's note

Art & Technology Publishing remains neutral with regard to jurisdictional claims in published maps and institutional affiliations.